

EXTENT OF SOLID SOLUTION IN Pb-Sn AND Sb-Bi CHALCOGENIDES

HUIFANG LIU

Department of Geology, University of Maryland, College Park, Maryland 20742, U.S.A.

CHARLES R. KNOWLES

Idaho Geological Survey, University of Idaho, Moscow, Idaho 83843, U.S.A.

LUKE L. Y. CHANG

Department of Geology, University of Maryland, College Park, Maryland 20742, U.S.A.

ABSTRACT

The systems of Pb-Sn and Sb-Bi chalcogenides were examined for the formation of solid solutions. In the system PbS - PbSe - SnS - SnSe at 500°C, both cubic (NaCl-type) and orthorhombic (GeS-type) solid solutions are extensive, whereas in the system PbSe - PbTe - SnSe - SnTe, the cubic solid-solution is the dominant phase, and the orthorhombic solid-solution is limited to the SnSe corner. Between Pb-Sn sulfides and tellurides, ranges of solid solution are restricted. In the Sb-Bi chalcogenides, the systems Sb₂S₃ - Sb₂Se₃ - Bi₂S₃ - Bi₂Se₃ and Sb₂Se₃ - Sb₂Te₃ - Bi₂Se₃ - Bi₂Te₃ at 500°C are characterized by extensive orthorhombic and hexagonal solid-solutions, respectively. Tetradymite is stable in the system Sb₂S₃ - Sb₂Te₃ - Bi₂S₃ - Bi₂Te₃ at 500°C. Several ranges of solid solutions that form in these systems cannot be successfully explained by using ionic size and electronegativity, the traditional parameters. R_{π} and R_{σ} of St. John & Bloch (1974) are used to differentiate between NaCl- and GeS-type structures in the case of Pb-Sn chalcogenides and between stibnite- and tetradymite-type structures in the case of Sb-Bi chalcogenides. The two parameters are defined by r_s and r_p , the radii of the s and p orbitals. For a bond between atoms A and B, they can be calculated as follows:

$$R_{\pi}^{AB} = R_{\pi}^A + R_{\pi}^B = (r_p^A + r_s^A) + (r_p^B - r_s^B)$$

and

$$R_{\sigma}^{AB} = R_{\sigma}^A + R_{\sigma}^B = (r_s^A + r_p^A) - (r_s^B + r_p^B).$$

Keywords: solid solution, Pb-Sn, Bi-Sb, chalcogenide, structure type.

SOMMAIRE

Nous avons étudié l'étendue des solutions solides dans les systèmes de chalcogénures à Pb-Sn et à Sb-Bi. Dans le système PbS - PbSe - SnS - SnSe à 500°C, deux solutions solides, cubique (structure du NaCl) et orthorhombique (structure du GeS), occupent une grande étendue, tandis que dans le système PbSe - PbTe - SnSe - SnTe, la solution solide cubique est dominante, et la solution solide orthorhombique est limitée aux compositions riches en SnSe. Entre les sulfures et les tellurures à Pb-Sn, l'étendue des solutions solides est limitée. Dans le cas des chalcogénures à Sb-Bi, les systèmes Sb₂S₃ - Sb₂Se₃ - Bi₂S₃ - Bi₂Se₃ et Sb₂Se₃ - Sb₂Te₃ - Bi₂Se₃ - Bi₂Te₃ à 500°C montrent une large étendue des champs de solution solide orthorhombique et hexagonale, respectivement. La tétradymite est stable dans le système Sb₂S₃ - Sb₂Te₃ - Bi₂S₃ - Bi₂Te₃ à 500°C. Dans plusieurs cas, les paramètres traditionnels, rayon ionique et électronégativité, ne semblent pas utiles pour expliquer l'étendue des solutions solides. Nous nous servons plutôt des paramètres R_{π} et R_{σ} de St. John et Bloch (1974) pour différencier dans les chalcogénures à Pb-Sn, ceux qui adoptent les structures de type NaCl et GeS, respectivement, et dans les chalcogénures à Sb-Bi, ceux qui adoptent les structures de type stibnite et tétradymite, respectivement. Ces deux paramètres dépendent de r_s et r_p , les rayons des orbites s et p ; pour une liaison entre les atomes A et B, ils sont définis comme suit:

$$R_{\pi}^{AB} = R_{\pi}^A + R_{\pi}^B = (r_p^A + r_s^A) + (r_p^B - r_s^B)$$

$$R_{\sigma}^{AB} = R_{\sigma}^A + R_{\sigma}^B = (r_s^A + r_p^A) - (r_s^B + r_p^B).$$

Mots-clés: solution solide, Pb-Sn, Bi-Sb, chalcogénure, type de structure.

INTRODUCTION

Pb–Sn and Sb–Bi are two pairs of elements that exhibit many similarities in crystallochemical properties such as ionization potential, electronegativity, and both ionic and covalent radii (Wells 1984). They are thus considered in each case as similar cations in the formation of compounds and solid solutions. There are, however, some differences. The most distinct one is that Sn exists in both divalent and tetravalent states and forms SnX , Sn_2X_3 and SnX_2 with chalcogenide elements, whereas PbX is the only type of lead chalcogenide. Both Sb and Bi form chalcogenides, Sb_2X_3 or Bi_2X_3 , but they crystallize with two distinct structural types.

The similarity and contrast of Pb–Sn and Sb–Bi in chalcogenides were examined in the systems $\text{PbS} - \text{SnS} - \text{PbSe} - \text{SnSe}$, $\text{PbSe} - \text{SnSe} - \text{PbTe} - \text{SnTe}$, $\text{PbS} - \text{SnS} - \text{PbTe} - \text{SnTe}$, $\text{Bi}_2\text{S}_3 - \text{Sb}_2\text{S}_3 - \text{Bi}_2\text{Se}_3 - \text{Sb}_2\text{Se}_3$, $\text{Bi}_2\text{Se}_3 - \text{Sb}_2\text{Se}_3 - \text{Bi}_2\text{Te}_3 - \text{Sb}_2\text{Te}_3$, and $\text{Bi}_2\text{S}_3 - \text{Sb}_2\text{S}_3 - \text{Bi}_2\text{Te}_3 - \text{Sb}_2\text{Te}_3$. End members of the systems under consideration that occur in nature include galena (PbS), clausthalite (PbSe), altaite (PbTe), herzenbergite (SnS), stibnite (Sb_2S_3), telluroantimonite (Sb_2Te_3) (Chizhikov & Shchastliviy 1970), bismuthinite (Bi_2S_3), guanajuatite and paraguanajuatite (Bi_2Se_3) (Earley 1950, Chizhikov & Shchastliviy 1968), tellurobismuthite (Bi_2Te_3) (Chizhikov & Shchastliviy 1970). Other minerals with reported compositions in the systems are teallite (Chang & Brice 1971), tetradyomite (Harker 1934), kawazulite (Miller 1981) and skippenite (Johan *et al.* 1987).

EXPERIMENTAL PROCEDURES

Starting compositions were prepared from reagent-

grade lead, tin, antimony, bismuth, sulfur, selenium, and tellurium; all have 99.95% purity or better. Heat treatment was made in electric furnaces in which the temperatures were controlled to within $\pm 2^\circ\text{C}$, and the conventional technique of sealed, evacuated glass capsule (Kullerud & Yoder 1959) was used. Generally, the duration of treatment ranged from 60 days at 500°C to 1 day at 900°C and above. At the end of the heat treatment, the samples were quenched with compressed air. As a test of equilibrium, some samples were heated to complete melting, quenched, ground under acetone, and annealed at the desired temperatures for the same length of time as their counterparts. If the final assemblages showed no differences caused by changing the procedure, equilibrium is assumed to have been attained.

X-ray powder diffraction, reflected-light microscopy and electron-microprobe analysis were used for phase characterization. Cell dimensions were computed with a least-squares refinement program (Benoit 1987). Solidus and liquidus were drawn on the basis of microscopic observations. The error is estimated to be less than 2.5°C . Phase boundaries in the subsolidus region were constructed by both parametric and phase-disappearance methods (Cullity 1956).

THE Pb–Sn CHALCOGENIDES

Phase relations along the binary joins

All PbX have the NaCl-type structure, whereas SnX chalcogenides crystallize with either GeS- or NaCl-type structure (Wiedemeier & von Schnering 1978). For the three $\text{PbX}_1 - \text{PbX}_2 - \text{SnX}_1 - \text{SnX}_2$ monochalcogenide systems (X_1 and X_2 are used to represent any two of the three chalcogen elements, S, Se, and Te), there are nine boundary joins. Among lead chalc-

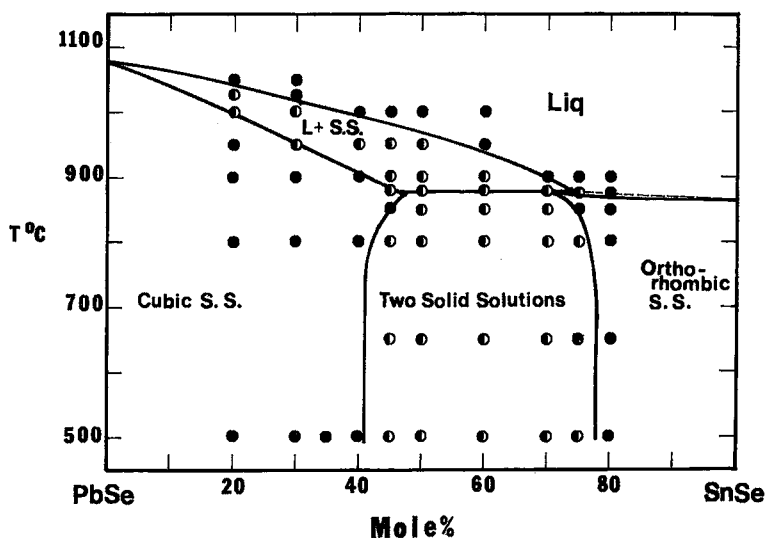


FIG. 1. Phase relations along the join $\text{PbSe} - \text{SnSe}$. Solid circle and half-filled circle represent one- and two-phase assemblages, respectively.

genides and among tin chalcogenides, equilibrium relations have been established. Complete series of solid solutions exist along the joins PbS-PbSe, PbSe-PbTe (Liu & Chang 1994) and SnS-SnSe (Liu & Chang 1992), eutectic relations with and without extensive terminal solid-solutions are present along the joins SnSe-SnTe and SnS-SnTe (Liu & Chang 1992), respectively, and an immiscibility dome characterizes the join PbS-PbTe (Liu & Chang 1994).

Equilibrium relations along the join PbS-SnS were studied extensively because of the presence of teallite (PbSnS_2) in nature. Krebs & Langner (1964) proposed two ranges of solid solution, separated by a two-phase region with compositions from 90 to 55 mol% PbS. Kuznetsov & Li (1964) established a solid solution series ranging from 30 to 53 mol% PbS, and confirmed the existence of PbSnS_2 . An equilibrium study by Chang & Brice (1971) showed that between SnS and PbSnS_2 , a complete series of solid solutions exists, with melting temperature decreasing from 875°C for SnS (herzenbergite) to 725°C for PbSnS_2 (teallite). A eutectic relation exists between PbSnS_2 and PbS (Chang 1987). Above 600°C, SnS has a nonquenchable phase-transition (Moh 1969).

Along the join PbSe-SnSe, Woolley & Berolo (1968) established the boundaries of PbSe-based solid solutions, $\text{Pb}_{1-x}\text{Sn}_x\text{Se}$, above 700°C, with x equal to 0.425 at 870°C, 0.390 at 800°C, and 0.385 at 700°C. Two terminal solid-solutions were defined above 800°C by Latypov *et al.* (1971), separated by a two-phase region extending from 37 to 82 mol% SnSe. The join was found to have a peritectic point at 880°C and approximately 70 mol% SnSe. Results from the present study (Fig. 1) correlate well with previous determinations, and extend phase relations to 500°C. The cubic solid-solution has ranges extending to 41 mol% SnSe at 500°C and 48 mol% SnSe at 880°C, the peritectic temperature. The ranges of the orthorhombic solid-solution vary from 78 mol% SnSe at 500°C to 72 mol% SnSe at 880°C. The separation between solidus and the liquidus in the compositions richer than 75 mol% SnSe is too narrow to be experimentally detectable.

A complete solid-solution series of the NaCl-type structure exists along the join PbTe-SnTe (Abrikosov *et al.* 1958, Hiscocks & West 1968).

Phase relations in the systems of Pb-Sn chalcogenides

Phase relations in the system PbS - PbSe - SnS - SnSe at 500°C are shown in Figure 2a. Two series of

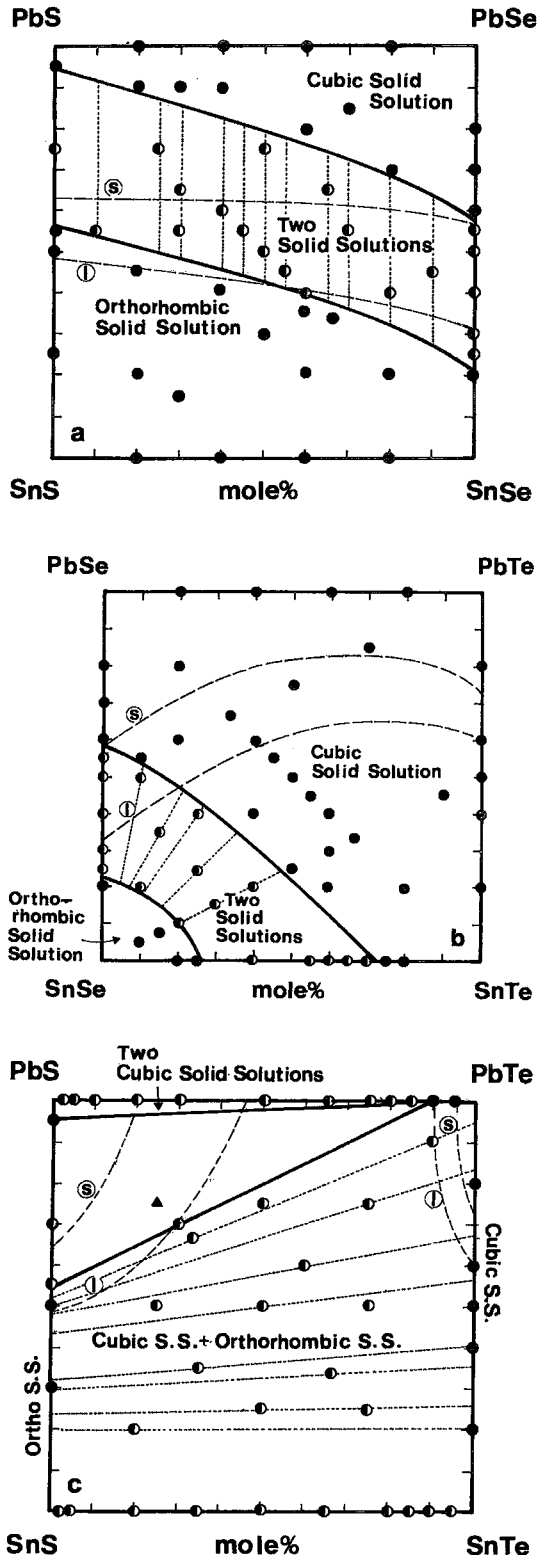


FIG. 2. Phase relations at 500°C in the systems (a) PbS - PbSe - SnS - SnSe, (b) PbSe - PbTe - SnSe - SnTe and (c) PbS - PbTe - SnS - SnTe. Liquid-solid equilibria at 900°C also are shown and represented by dashed lines. The "s" denotes the solidus, and the "l", liquidus. Tie lines in the two-phase region are represented by dotted lines.

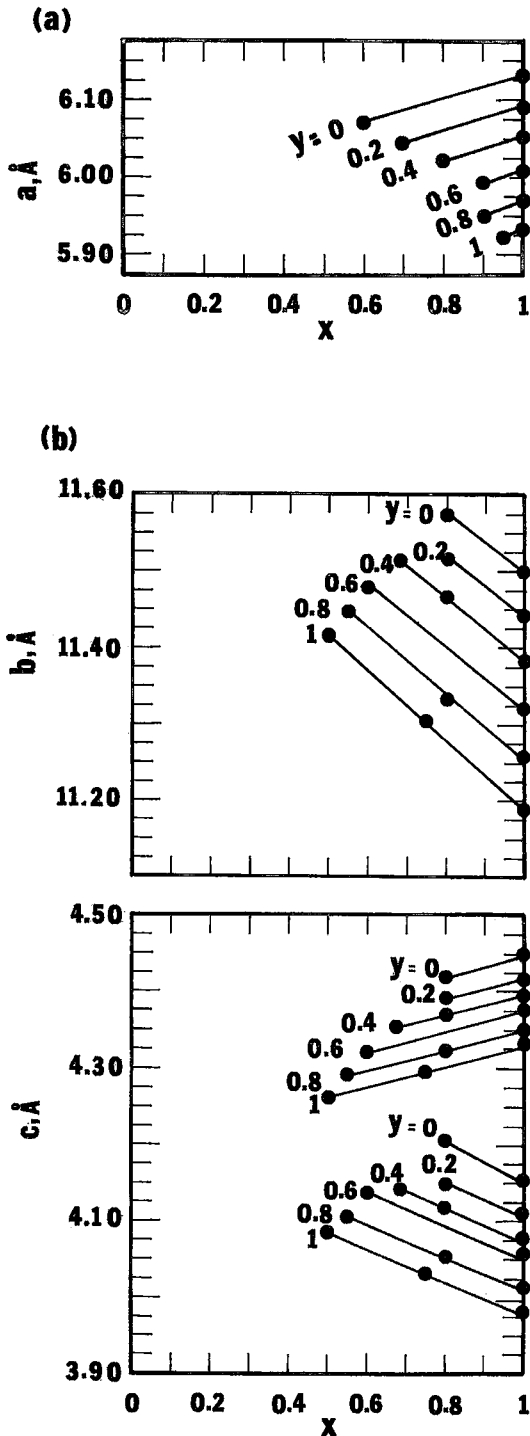


FIG. 3. Variations of cell dimensions with composition for (a) cubic $Pb_xSn_{1-x}S_ySe_{1-y}$, and (b) orthorhombic $Pb_xSn_{1-x}S_ySe_{1-y}$ solid solutions. Estimated standard errors are ≤ 0.003 Å for a and c , and ≤ 0.005 Å for b .

solid solution exist, a cubic solid-solution along the PbS–PbSe series and an orthorhombic solid-solution along the SnS–SnSe series. The boundary lines that delimit the ranges of both series in the system demonstrate that substitution between lead and tin in the presence of both sulfur and selenium follows the same trend as that established along the binary joins PbS–SnS and PbSe–SnSe. With an increase in Se content, the amount of tin in the cubic solid-solution increases, and the amount of lead in the orthorhombic solid-solution decreases. Also shown in Figure 2a are liquid–solid equilibria at 900°C. The preferred substitution of Pb by Sn in the selenide-rich solid-solution becomes less significant. Cell dimensions of both cubic and orthorhombic solid-solutions were calculated, their variations with composition in the system are shown in Figure 3. The a dimension of the cubic solid-solution decreases with increase in sulfur and tin contents. In the orthorhombic series, an increase in S content causes a decrease in a , b , and c dimensions, whereas an increase in Sn content causes a decrease in a , but an increase in b and c .

Phase relations in the system PbSe – PbTe – SnSe – SnTe are shown in Figure 2b. At 500°C, the system consists of two solid-solution series, as in the preceding system. The orthorhombic solid-solution, however, occupies only a small region restricted to the SnSe corner. At 900°C, liquid dominates the system, and forms a two-phase assemblage with the cubic solid-solution, which reduces its range to the Pb-rich region. The cell dimension of the cubic solid-solution decreases linearly as the content of Sn and Se increases (Fig. 4).

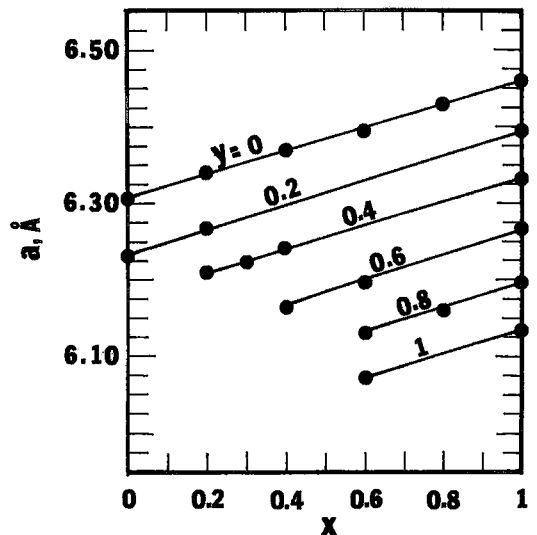


FIG. 4. Variations of cell dimensions with composition for the cubic $Pb_xSn_{1-x}S_ySe_{1-y}$ solid solution. Estimated standard error is ≤ 0.003 Å for a .

The system PbS - PbTe - SnS - SnTe is characterized by the presence of a three-phase region that consists of two cubic solid-solutions and an orthorhombic solid-solution at 500°C (Fig. 2c). The ranges of solid solution, 9 mol% PbTe in SnS and 19 mol% SnS in PbTe at 500°C, as estimated by Matyas (1985), were not confirmed. Experimental data obtained in the present study demonstrate the absence of solid solution along the join PbS-SnTe, although Matyas & Borisenko (1990) proposed 30 mol% PbS in SnTe and 20 mol% SnTe in PbS at 500°C. At 900°C, cubic solid-solutions are stable only at the PbS and PbTe corners.

THE Bi-Sb CHALCOGENIDES

Phase relations along the boundary joins

The six simple stoichiometric chalcogenides of Sb and Bi can be divided into two groups: the orthorhombic stibnite-type (Sb_2S_3 , Sb_2Se_3 and Bi_2S_3) structures and the hexagonal, tetradymite-type (Sb_2Te_3 , Bi_2Se_3 and Bi_2Te_3) structures.

Sb_2S_3 and Sb_2Se_3 form a complete solid-solution series; a minimum on its solidus and liquidus at 550°C and 70 mol% Sb_2S_3 was found in the present study, which correlates well with results of Ivlieva & Abrikosov (1964). Variations of cell dimensions show that a has a linear relation, b has a positive deviation, and c has a negative deviation with composition. Phase relations along the join Sb_2S_3 - Sb_2Te_3 from the present study illustrate a simple eutectic relation with a eutectic point at 82.5 mol% Sb_2S_3 and 480°C, which are different from previously published results of Ivlieva (1971) and Gospodinov *et al.* (1974). The former proposed the existence of a "δ"-phase that has an excess of Sb over that in stoichiometric Sb_2Te_3 in equilibrium with liquid, whereas the latter reported the existence of a solid solution that extends from Sb_2S_3 to 30 mol% Sb_2Te_3 at 450°C. The join Sb_2Se_3 - Sb_2Te_3 has been studied by several investigators. Ivlieva & Abrikosov (1964) established a eutectic relation with a eutectic point at 18 mol% Sb_2Te_3 and 500°C. Two solid-solution series exist at 560°C, one from Sb_2Se_3 to $Sb_2(Se_{0.95}Te_{0.05})_{23}$ and the other from Sb_2Te_3 to $Sb_2(Se_{0.66}Te_{0.34})_{23}$. Palkina & Kuznetsov (1965) reported a miscibility gap between 46.5 and 97 mol% Sb_2Se_3 at 500°C along this join. An ordered phase of composition Sb_2SeTe_2 was reported by Molodkin *et al.* (1979) on the basis of measurements of thermal conductivity and electrical conductivity, although superlattice reflections were not observed in X-ray powder diffraction. Andriamihaja *et al.* (1985) found two solid-solution series over the ranges of $0 \leq x \leq 1$ and $1 \leq x \leq 2$ of the $Sb_2Se_xTe_{3-x}$, both based on the Sb_2Te_3 structure but differing in space groups ($R\bar{3}m$ and $R3m$). Results obtained in the present study are shown in Figure 5a, with the Sb_2Te_3 -based solid-

solution series extending to 45 mol% Sb_2Se_3 , and the Sb_2Se_3 -based solid-solution series extending to 10 mol% Sb_2Te_3 . Both a and c dimensions decrease with increasing Se content and show a negative deviation from Vegard's law.

Phase relations along the join Bi_2S_3 - Bi_2Se_3 are shown in Figure 5b. Between two series of solid solutions, there exists a eutectic relation with a eutectic point at 680°C and 23 mol% Bi_2S_3 . The orthorhombic series extends to 70 mol% Bi_2Se_3 at 690°C and to 63 mol% Bi_2Se_3 at 300°C, whereas the ranges of the hexagonal series are from Bi_2Se_3 to 19 mol% Bi_2S_3 and from Bi_2Se_3 to 15 mol% Bi_2S_3 at 690° and 300°C, respectively. The phase relations established correlate in general with published results of Beglaryan & Abrikosov (1959), Godovikov & Nenashcheva (1966) and Neumann & Scheidegger (1967). Cell dimensions of both orthorhombic and hexagonal solid-solutions show a linear dependence on composition. Tetradymite is a stable phase along the join Bi_2S_3 - Bi_2Te_3 ; its composition varies from $Bi_2S_{1.2}Te_{1.8}$ to $Bi_2S_{Te_2}$. It forms a eutectic relation with each of Bi_2S_3 and Bi_2Te_3 . Invariant points occur at 620°C and 45.5 mol% Bi_2S_3 and 580°C and 90 mol% Bi_2Te_3 (Fig. 5c). Results match well with published data of Beglaryan & Abrikosov (1959) and Kuznetsov & Kanishcheva (1970), but are at variance with Glatz's (1967) results. The join Bi_2S_3 - Bi_2Te_3 , as interpreted by Glatz, consists of two compounds, a congruently melting γ -phase (γ -tetradymite) and an incongruently melting β -phase (β -tetradymite). Between Bi_2Se_3 and Bi_2Te_3 , a complete solid-solution series exists without maximum or minimum on the liquidus and solidus. Both a and c decrease from Bi_2Te_3 to Bi_2Se_3 , but a linear relation exists only in the a dimension. Several members of the solid-solution series have been reported in nature, including Bi_2Te_2Se , Bi_2TeSe_2 , $Bi_2Te_{1.5}Se_{1.5}$, $Bi_2Te_{1.55}Se_{1.45}$ and $Bi_2Te_{1.06}Se_{1.94}$ (Miller 1981). Kawazulite is an ordered tetradymite-type mineral of composition Bi_2Te_2Se , with Se occupying the S position (Bland & Basinski 1961). Although its crystal structure has not been determined, skippenite may have an ordered arrangement of Te and Se of the type $Bi_2(Te_{0.5}Se_{0.5})_2Se$. Neither kawazulite nor skippenite was synthesized in the present study at temperatures above 500°C.

Along the join Sb_2S_3 - Bi_2S_3 , there is a complete solid-solution series with monotonic solidus and liquidus (Bondar 1966, Springer & Laflamme 1971). Members of the solid-solution series along the join Sb_2Te_3 - Bi_2Te_3 melt over a very narrow interval of temperatures between 625°C (Sb_2Te_3) and 587°C (Bi_2Te_3). The melting curve seems to be monotonic and slightly convex. Bekebrede & Guentert (1962) and Abrikosov *et al.* (1979) reported comparable results. Smith *et al.* (1962), however, observed that the liquidus and solidus coincide at 33.3 and 66.7 mol% Sb_2Te_3 . Linear relations were observed between

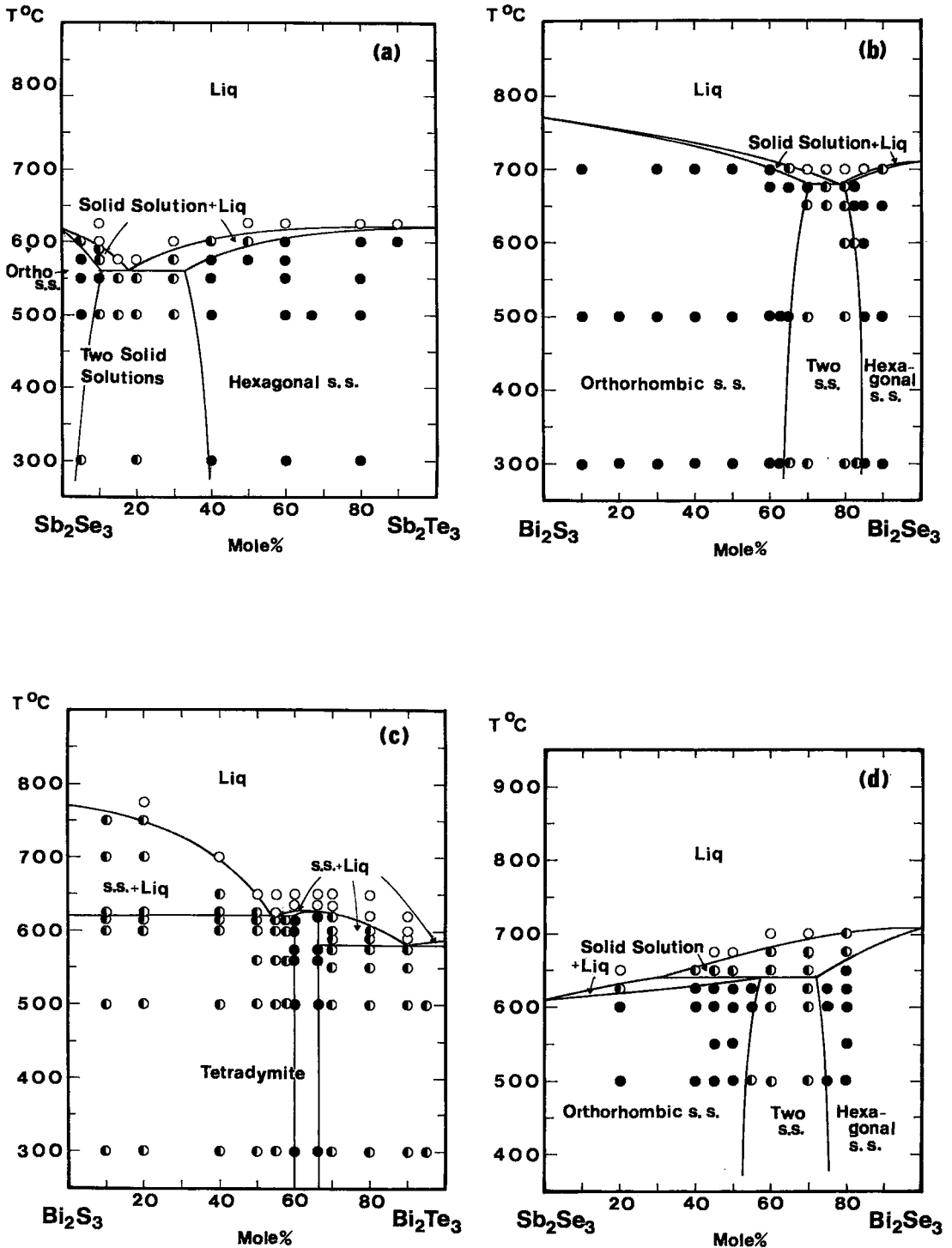


FIG. 5. Phase relations along the joins (a) Sb_2Se_3 - Sb_2Te_3 , (b) Bi_2S_3 - Bi_2Se_3 , (c) Bi_2S_3 - Bi_2Te_3 and (d) Sb_2Se_3 - Bi_2Se_3 . Open and solid circles represent liquid and solid phases, respectively, and half-filled circles represent two-phase assemblages.

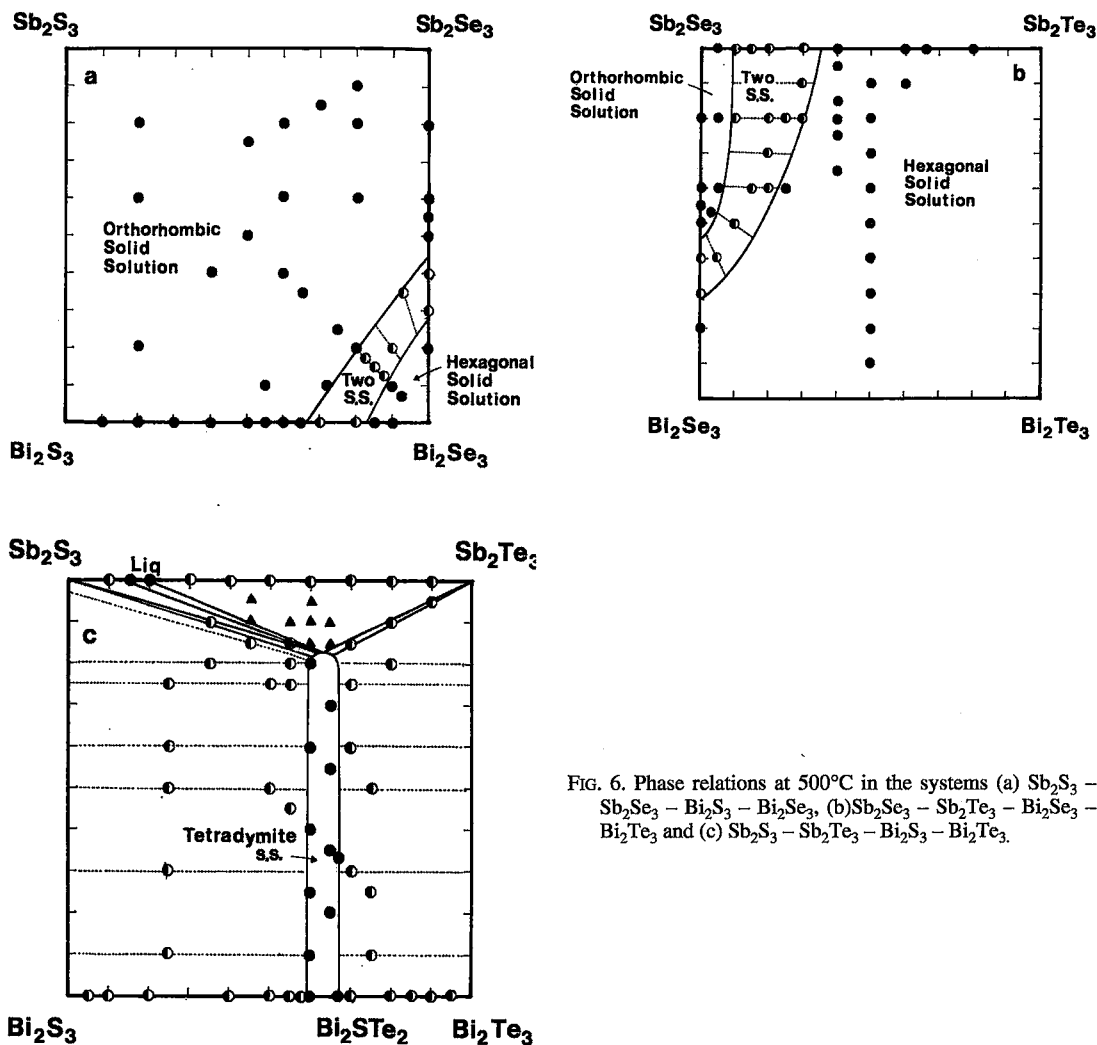


FIG. 6. Phase relations at 500°C in the systems (a) $\text{Sb}_2\text{S}_3 - \text{Sb}_2\text{Se}_3 - \text{Bi}_2\text{S}_3 - \text{Bi}_2\text{Se}_3$, (b) $\text{Sb}_2\text{Se}_3 - \text{Sb}_2\text{Te}_3 - \text{Bi}_2\text{Se}_3 - \text{Bi}_2\text{Te}_3$ and (c) $\text{Sb}_2\text{S}_3 - \text{Sb}_2\text{Te}_3 - \text{Bi}_2\text{S}_3 - \text{Bi}_2\text{Te}_3$.

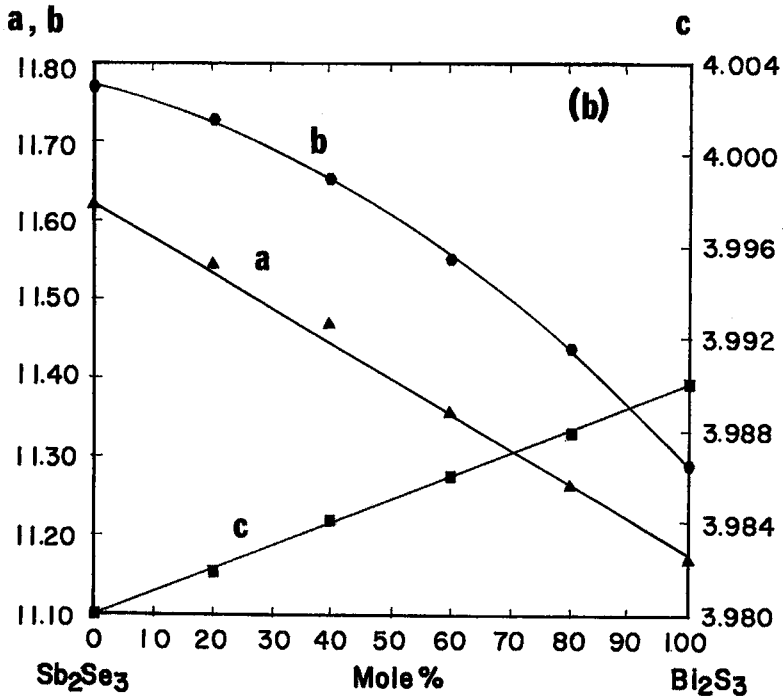
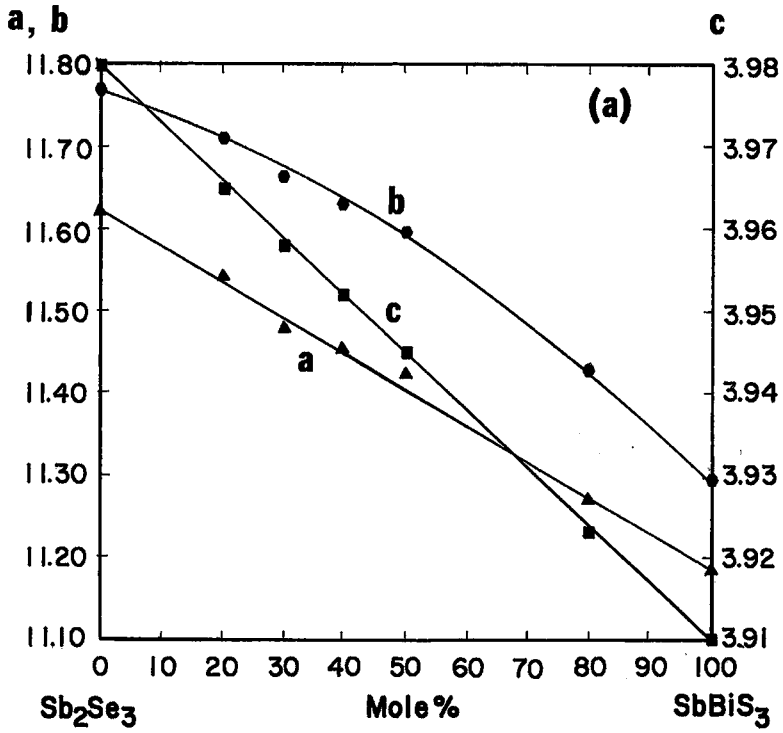
cell dimensions and composition along the joins $\text{Sb}_2\text{S}_3 - \text{Bi}_2\text{S}_3$ and $\text{Sb}_2\text{Te}_3 - \text{Bi}_2\text{Te}_3$. The join $\text{Sb}_2\text{Se}_3 - \text{Bi}_2\text{Se}_3$ consists of two solid-solution series, with the orthorhombic one ranging from Sb_2Se_3 to 53 mol% Bi_2Se_3 and the hexagonal one from Bi_2Se_3 to 25 mol% Sb_2Se_3 . A peritectic point was established at 640°C and 30 mol% Bi_2Se_3 (Fig. 5d). The cell dimensions in both series show a linear dependence on composition.

Phase relations in the systems of Sb-Bi chalcogenides

Phase relations in the system $\text{Sb}_2\text{S}_3 - \text{Sb}_2\text{Se}_3 - \text{Bi}_2\text{S}_3 - \text{Bi}_2\text{Se}_3$ at 500°C are shown in Figure 6a. The orthorhombic solid-solution, including three (Sb_2S_3 ,

Sb_2Se_3 , and Bi_2S_3) of the four end members, dominates the system with an extensive single-phase region, the limits of which may be represented by a line connecting $\text{Bi}_2(\text{S}_{0.35}\text{Se}_{0.65})_3$ along the join $\text{Bi}_2\text{S}_3 - \text{Bi}_2\text{Se}_3$ to $(\text{Sb}_{0.47}\text{Bi}_{0.53})_2\text{Se}_3$. The hexagonal solid-solution and a two-phase region exist beyond this line toward Bi_2Se_3 . The cell dimensions of the orthorhombic solid-solution in the system were measured along the joins $\text{Sb}_2\text{Se}_3 - \text{Bi}_2\text{S}_3$ (Fig. 7a).

In the system $\text{Sb}_2\text{Se}_3 - \text{Sb}_2\text{Te}_3 - \text{Bi}_2\text{Se}_3 - \text{Bi}_2\text{Te}_3$, members have the hexagonal structure except for Sb_2Se_3 . Therefore, the hexagonal solid-solution is the dominant phase (Fig. 6b), and its range may be delimited by a line connecting $(\text{Sb}_{0.28}\text{Bi}_{0.72})_2\text{Se}_3$ and $\text{Sb}_2(\text{Se}_{0.65}\text{Te}_{0.35})_3$. Thus three solid solutions exist beyond this line toward Sb_2Se_3 . The cell dimensions



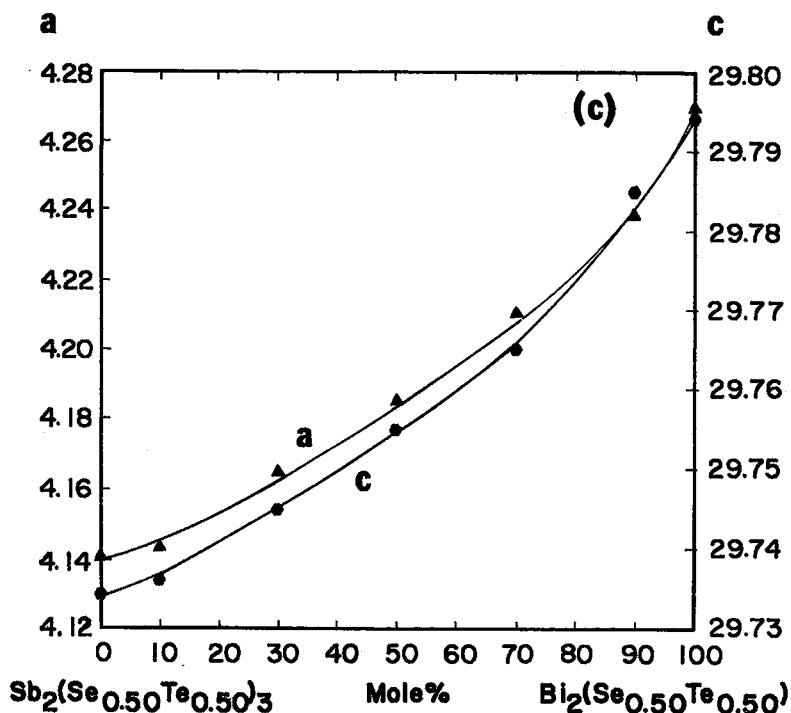


FIG. 7. Variations of cell dimensions (in Å) with composition along the joins (a) $\text{Sb}_2\text{Se}_3\text{-SbBiS}_3$, (b) $\text{Sb}_2\text{Se}_3\text{-Bi}_2\text{S}_3$, and (c) $\text{Sb}_2(\text{Se}_{0.50}\text{Te}_{0.50})_3\text{-Bi}_2(\text{Se}_{0.50}\text{Te}_{0.50})_3$. Estimated standard errors are ≤ 0.003 Å for *a* and *c* in (a) and (b), and ≤ 0.003 Å for *a* and ≤ 0.005 Å for *c* in (c).

were measured along the join $\text{Sb}_2(\text{Se}_{0.50}\text{Te}_{0.50})_3\text{-Bi}_2(\text{Se}_{0.50}\text{Te}_{0.50})_3$ to assess their dependence on composition. Both curves as shown in Figure 7b illustrate a negative deviation from linearity.

Phase relations in the system $\text{Sb}_2\text{S}_3\text{-Sb}_2\text{Te}_3\text{-Bi}_2\text{S}_3\text{-Bi}_2\text{Te}_3$ are characterized by the presence of tetradymite (Fig. 6c). With a constant S/Te ratio, Sb replaces Bi in tetradymite, to an extent of 83 mol%, which forms equilibrium assemblages with Sb_2S_3 , Sb_2Te_3 and the liquid phase stable along the join $\text{Sb}_2\text{S}_3\text{-Sb}_2\text{Te}_3$. A tetradymite-based solid solution exists in equilibrium with $(\text{Sb}_x\text{Bi}_{1-x})_2\text{S}_3$ solid solution in the sulfur-rich region, and with $(\text{Sb}_x\text{Bi}_{1-x})_2\text{Te}_3$ solid solution in the tellurium-rich region. The variation of cell dimensions with composition of the tetradymite solid-solution is shown in Figure 8.

DISCUSSION OF RESULTS

The phase relations established have demonstrated that Sn and Pb do substitute for each other in their sulfides, selenides, and tellurides, as expected from the similarities in their crystallochemical parameters.

However, there are distinctions in the extent of their substitutions. Along the join PbS-SnS , SnS can take up to 55 mol% PbS, whereas only 5 mol% SnS can be accommodated by PbS (Fig. 2a). These extents of substitutions are not expected, judging from the relative sizes of Pb^{2+} and Sn^{2+} , because Sn^{2+} is smaller than Pb^{2+} and should more easily go into the structure of PbS than Pb^{2+} into the structure of SnS.

In the systems $\text{Sb}_2\text{S}_3\text{-Sb}_2\text{Se}_3\text{-Bi}_2\text{S}_3\text{-Bi}_2\text{Se}_3$ and $\text{Sb}_2\text{Se}_3\text{-Sb}_2\text{Te}_3\text{-Bi}_2\text{Se}_3\text{-Bi}_2\text{Te}_3$ (Figs. 5, 6), the phase relations established illustrate the fact that in the presence of a similar pair of cations (Sb-Bi) and anions (S-Se and Se-Te), extensive ranges of solid solutions can be expected. Distinct features established are: (1) the solubility of Bi_2Se_3 in Sb_2Se_3 is greater than that of Sb_2Se_3 in Bi_2Se_3 , although the ionic radius of Bi is larger than that of Sb, (2) the solubility of Bi_2Se_3 in Bi_2S_3 is greater than that of Bi_2S_3 in Bi_2Se_3 , although the ionic radius of Se is larger than that of S, and (3) the solubility of Bi_2Se_3 in Sb_2S_3 is greater than that of Sb_2S_3 in Bi_2Se_3 , although the ionic radii of Bi and Se are larger than those of Sb and S, respectively.

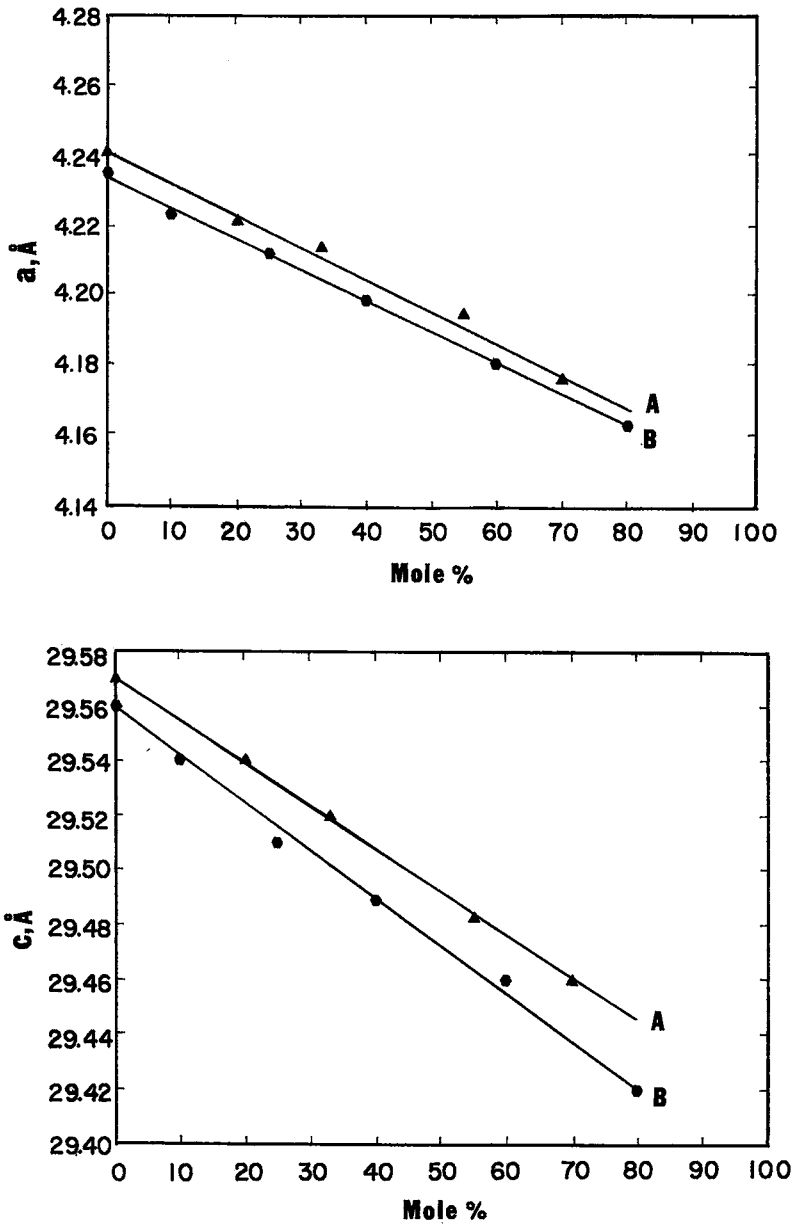


FIG. 8. Variations of cell dimensions a (top) and c (bottom) with composition for tetradymite-based solid solutions: (A) Bi_2STe_2 -“ Sb_2STe_2 ” series, and (B) $\text{Bi}_2\text{S}_{1.2}\text{Te}_{1.8}$ -“ $\text{Sb}_2\text{S}_{1.2}\text{Te}_{1.8}$ ” series. Estimated standard errors are ≤ 0.003 Å for a and ≤ 0.005 Å for c .

The “abnormal” substitutions illustrated in the systems cannot be successfully explained by utilizing the traditional parameters, *i.e.*, ionic radius and electronegativity. Ionic size has been successfully used in prediction of coordination number of the atoms in ionic compounds, but not so for covalent

compounds, especially when fractional bonds are involved. The difference in electronegativity (ΔE) has been used in estimating ionocovalent character of the bonds, with a smaller ΔE for a higher covalency (Megaw 1973, Wells 1984).

On the basis of calculated radii of the s and p

orbitals, St. John & Bloch (1974) introduced two parameters, R_G and R_π . For a bond between atoms A and B, the two parameters are calculated as:

$$R_G^{AB} = R_G^A + R_G^B = (r_s^A + r_p^A) - (r_s^B + r_p^B) \quad (1)$$

and

$$R_\pi^{AB} = R_\pi^A + R_\pi^B = (r_p^A + r_s^A) + (r_p^B - r_s^B) \quad (2)$$

where r_s and r_p are the radii of the s and p orbitals.

According to equation (1), R_G (R_G^A and R_G^B) increases with the size of an atom and is a measure of its ability to capture available electrons. Therefore, R_G^{AB} reaches a maximum when the bond is strongly ionic and should characterize the ionocovalent character of a bond. Its function is thus analogous to ΔE . R_π^A and R_π^B in equation (2) measure the difference in radius of the s and p orbitals and can be used to characterize the degree of s - p hybridization. Where R_π^{AB} is large, s - p hybridization is difficult, and the bond will be of p -type. Where these p -orbitals are not fully filled, resonance occurs. The bonding may thus be considered as delocalized and covalent, as an electron-density map of PbS shows (Noda *et al.* 1983), or it has some metallic character. Therefore, R_π^{AB} can be used as a measure of the covalometallic character, where only s and p orbitals are involved. By using R_π and R_G , Porte (1983) constructed a structural map to differentiate NaCl-, GeS-, P(black)-, TII- and CsCl-type compounds.

The structure types, coordinations, ΔE and ionic radius ratios of PbX, SnX, Sb₂X₃ and Bi₂X₃ (X: S, Se and Te) are listed in Table 1. The values of ΔE (Bloch

& Schatteman 1981) of the pairs PbS-SnS, PbSe-SnSe and Sb₂Se₃-Bi₂Se₃ are nearly the same, and their respective ratios of ionic radii (Shannon & Prewitt 1969) also are very close. Yet each pair shows different coordination numbers and crystal structures. PbS and PbSe have the NaCl-type structure, whereas SnS and SnSe crystallize with the GeS-type structure. In the GeS-type structure (Wiedemeier & von Schnering 1978), a 3+3+1 coordination in the form of a distorted octahedron exists. Sn has three sulfur atoms at 2.665, 2.665, 2.627 Å, three at 3.290, 3.290, 3.388 Å, and one at 4.093 Å in SnS, and three selenium atoms at 2.793, 2.793, 2.744 Å, three at 3.343, 3.343, 3.468 Å, and one at 4.103 Å in SnSe. In relation to the NaCl-type, the GeS-type structure can be transformed by a shift of $a/2$ to a NaCl-type arrangement. Sb₂Se₃ has the stibnite-type structure (Bayliss & Nowacki 1972), whereas Bi₂Se₃ crystallizes with the tetradymite-type structure (Harker 1934). In Sb₂Se₃ (Tideswell *et al.* 1957, Voutsas *et al.* 1985), Sb occupies two structural positions. The first Sb-polyhedron has three selenium atoms at 2.66 Å, three at 3.22 to 3.26 Å, and one at 3.74 Å, which is identical to the Sn polyhedron in SnS and SnSe; the second Sb-polyhedron has one Se atom at 2.58 Å, two at 2.78 Å, two at 2.98 Å, and two at 3.46 Å, which may be considered as a 5 + 2 coordination. In the tetradymite structure, Bi has an octahedrally coordinated group.

Figure 9 illustrates the $R_\pi^{AB} - R_G^{AB}$ relationship of these chalcogenides. As shown, the structural transitions in these compounds are mainly caused by the change in covalometallic character, and ionocovalency may not play even a minor role in the transition from the GeS- to the NaCl-type. Therefore, ΔE is not sufficient to characterize the structure and bonding of the compounds in these cases. Figure 9 also shows that the metallic character of the bonding increases from stibnite- to galena-type structures. In these structures, the nature of the bonding changes from sp^3 hybridization to delocalized p -bonding, which is manifested by the three bonds + one lone-pair coordination in the former case (Bayliss & Nowacki 1972) and the regular octahedral coordination in the latter case (Wells 1984, Olivier-Fourcade *et al.* 1990). The GeS- and tetradymite-type structures have similar range of R_π^{AB} values. The difference in their coordination numbers is also very small.

The transition between NaCl- and GeS-type structures in Pb-Sn chalcogenides is mainly caused by covalometallic character (R_π^{AB}), with the bonding in the NaCl-type structures being more metallic. Because of the small R_π^{AB} value for Sn-S, it is very difficult for SnS to be accommodated by the NaCl-type structure. On the other hand, PbS is at the boundary between NaCl- and GeS-type structures. Therefore, it readily goes into the solid solution based upon the SnS structure.

The transition between tetradymite- and stibnite-

TABLE 1. STRUCTURE TYPES, COORDINATION NUMBERS, VALUES OF ΔE , AND RADIUS RATIOS OF Sn, Pb, Sb AND Bi CHALCOGENIDES

	S	Se	Te
Sn	GeS	GeS	NaCl
Structure Type	GeS	GeS	NaCl
C.N.	3+3+1	3+3+1	6
ΔE	0.77	0.56	0.39
r_c/r_a	0.51	0.47	0.42
Pb	NaCl	NaCl	NaCl
Structure Type	NaCl	NaCl	NaCl
C.N.	6	6	6
ΔE	0.76	0.55	0.38
r_c/r_a	0.65	0.60	0.54
Sb	Stibnite	Stibnite	Tetradymite
Structure Type	Stibnite	Stibnite	Tetradymite
C.N.	3+3+1 & 5+2	3+3+1 & 5+2	6
ΔE	0.57	0.36	0.19
r_c/r_a	0.41	0.38	0.34
Bi	Stibnite	Tetradymite	Tetradymite
Structure Type	Stibnite	Tetradymite	Tetradymite
C.N.	3+3+1 & 5+2	6	6
ΔE	0.61	0.40	0.23
r_c/r_a	0.52	0.48	0.43

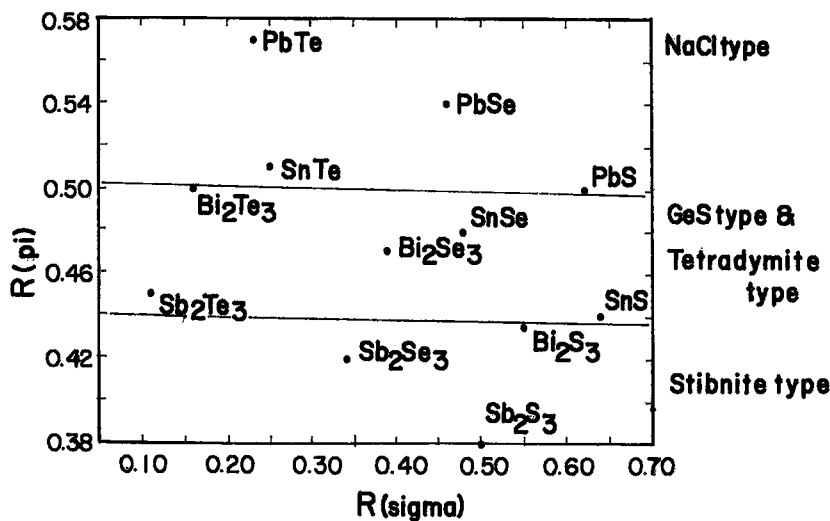


FIG. 9. $R_{\pi}^{AB} - R_{\sigma}^{AB}$ for Pb-, Sn-, Sb-, and Bi-chalcogenides.

type structures is also mainly caused by the covalent-metallic character (R_{π}^{AB}). Bi_2Se_3 must have a value of R_{π}^{AB} close to the structural boundary, so it crystallizes with the tetradymite structure and can be readily accommodated by the stibnite-type structure.

ACKNOWLEDGEMENTS

We are indebted to Dr. Y. Moëlo (Université de Nantes), Dr. Tonči B. Žunič (University of Copenhagen) and an anonymous referee for reviewing the manuscript. Thanks are due to Dr. Jack Tossell (University of Maryland) for his interest in this study and for his reading of this manuscript.

REFERENCES

- ABRIKOSOV, N.KH., BANKINA, V.F., KOLOMOETS, L.A. & ARATYUNOVA, L.L. (1979): Properties of solid solutions of bismuth and antimony chalcogenides during formation of ordered structure. *Russ. Inorg. Mater. (Izv. Akad. Nauk SSSR, Neorg. Mater.)* **15**, 400-402.
- , DYUL'DINA, K.A. & DANILYAN, T.A. (1958): The SnTe-PbTe system. *Russ. J. Inorg. Chem.* **3**, 1632-1636.
- ANDRIAMIHAJA, A., IBANEZ, A., JUMAS, J.C., OLIVIER-FOURCADE, J. & PHILIPPOT, E. (1985): Evolution structurale de la solution solide $\text{Sb}_2\text{Te}_{3-x}\text{Se}_x$ ($0 \leq x \leq 2$) dans le système $\text{Sb}_2\text{Te}_3 - \text{Sb}_2\text{Se}_3$. *Rev. Chim. Minérale* **22**, 357-368.
- BAYLISS, P. & NOWACKI, W. (1972): Refinement of the crystal structure of stibnite, Sb_2S_3 . *Z. Kristallogr.* **135**, 308-315.
- BEGLARYAN, M.L. & ABRIKOSOV, N.KH. (1959): The $\text{Bi}_2\text{Se}_3 - \text{Bi}_2\text{S}_3$ system. *Dokl. Akad. Nauk SSSR* **128**, 345-347 (in Russ.).
- BEKEBREDE, W.R. & GUENTERT, O.J. (1962): Lattice parameters in the system antimony telluride-bismuth telluride. *J. Phys. Chem. Solids* **23**, 1023-1025.
- BENOIT, P.H. (1987): Adaption to microcomputer of the Appleman-Evans program for indexing and least-squares refinement of powder-diffraction data for unit cell dimensions. *Am. Mineral.* **72**, 1018-1019.
- BLAND, J.A. & BASINSKI, S.J. (1961): The crystal structure of $\text{Bi}_2\text{Te}_2\text{Se}$. *Can. J. Phys.* **39**, 1040-1043.
- BLOCH, A.N. & SCHATTEMAN, G.C. (1981): Quantum-defect orbital radii and the structural chemistry of simple solids. In *Structure and Bonding in Crystals I* (M. O'Keeffe & A. Navrotsky, eds.). Academic Press, New York, N.Y. (49-72).
- BONDAR, N.M. (1966): Investigation of the system $\text{Bi}_2\text{S}_3 - \text{Sb}_2\text{S}_3$. *Russ. Inorg. Mater. (Izv. Akad. Nauk SSSR, Neorg. Mater.)* **2**, 1144-1147.
- CHANG, L.L.Y. (1987): Lead and tin substitution in sulfides. *Acta Geol. Taiwanica* **25**, 7-16.
- & BRICE, W.R. (1971): The herzenbergite-teallite series. *Mineral. Mag.* **38**, 186-189.
- CHIZHIKOV, D.M. & SHCHASTLIVYI, V.P. (1968): *Selenium and Selenides*. Collet Publishers, London, U.K.
- & ——— (1970): *Tellurium and Tellurides*. Collet Publishers, London, U.K.

- CULLITY, B.D. (1956): *Elements of X-ray Diffraction*. Addison-Wesley Publ. Co., Inc., Reading, U.K.
- EARLEY, J.W. (1950): Description and synthesis of selenide minerals. *Am. Mineral.* **35**, 337-364.
- GLATZ, A.C. (1967): The Bi_2Te_3 - Bi_2S_3 system and the synthesis of the mineral tetradymite. *Am. Mineral.* **52**, 161-170.
- GODOVIKOV, A.A. & NENASHEVA, S.N. (1966): X-ray diffraction study of the bismuth sulfide - bismuth selenide. *Mater. Genet. Eksp. Mineral.* **4**, 12-20 (in Russ.).
- GOSPODINOV, G.G., ODIN, I.N. & NOVOSELOVA, A.V. (1974): Solid solutions in anyimony(III) sulfide - antimony(III) telluride system. *Dokl. Bolg. Akad. Nauk* **27**, 1207-1209 (in Russ.).
- HARKER, D. (1934): The crystal structure of the mineral tetradymite, $\text{Bi}_2\text{Te}_2\text{S}$. *Z. Kristallogr.* **89**, 175-181.
- HISCOCKS, S.E.R. & WEST, P.D. (1968): Crystal pulling and constitution in $\text{Pb}_{1-x}\text{Sn}_x\text{Te}$. *J. Mater. Sci.* **3**, 76-79.
- IVLIEVA, V. I. (1971): The cross sections Sb_2Te_3 - Sb_2S_3 and $\text{Sb}_2\text{Te}_{2.9}$ - Sb_2S_3 of ternary system Sb-Te-S. *Russ. Inorg. Mater. (Izv. Akad. Nauk SSSR, Neorg. Mater.)* **7**, 1334-1337.
- _____ & ABRIKOSOV, N.KH. (1964): Phase relations in antimony chalcogenide systems. *Dokl. Akad. Nauk SSSR* **159**, 1326-1329 (in Russ.).
- JOHAN, Z., PICOT, P. & RUHLMANN, P. (1987): The ore mineralogy of the Otish Mountains uranium deposit, Quebec: skippenite, $\text{Bi}_2\text{Se}_2\text{Te}$ and watkinsonite, $\text{Cu}_2\text{PbBi}_4(\text{Se,S})_8$, two new mineral species. *Can. Mineral.* **25**, 625-638.
- KREBS, H. & LANGNER, D. (1964): Mischkristallsysteme zwischen halbleitenden Chalkogeniden der vierten Hauptgruppe II. *Z. anorg. allgem. Chem.* **334**, 37-49.
- KULLERUD, G. & YODER, H.S. (1959): Pyrite stability relations in the Fe-S system. *Econ. Geol.* **54**, 533-572.
- KUZNETSOV, V.G. & KANISHCHEVA, A.S. (1970): X-ray diffraction study of Bi_2Te_3 - Bi_2S_3 system. *Russ. Inorg. Mater. (Izv. Akad. Nauk SSSR, Neorg. Mater.)* **70**, 369-383.
- _____ & LI, CH'IH-FA (1964): X-ray diffraction investigation of the PbS - SnS system. *Russ. J. Inorg. Chem.* **9**, 656-659.
- LATYPOV, Z.M., SAVEL'EV, V.P. & AVER'YANOV, I.S. (1971): Lead selenide - tin(II) selenide system. *Russ. Inorg. Mater. (Izv. Akad. Nauk SSSR, Neorg. Mater.)* **7**, 1331-1333.
- LIU, HUIFANG & CHANG, L.L.Y. (1992): Phase relations in systems of tin chalcogenides. *J. Alloys & Compounds* **185**, 183-190.
- _____ & _____ (1994): Phase relations in the system PbS - PbSe - PbTe . *Mineral. Mag.* (in press).
- MATYAS, E.E. (1985): The system PbTe - SnS . *Russ. Inorg. Mater. (Izv. Akad. Nauk SSSR, Neorg. Mater.)* **21**, 144-145.
- _____ & BORISENKO, T.E. (1990): The lead monosulfide-tin monotelluride system. *Russ. Inorg. Mater. (Izv. Akad. Nauk SSSR, Neorg. Mater.)* **26**, 643-644.
- MEGAW, H.D. (1973): *Crystal Structures: a Working Approach*. W.B. Saunders Co., Philadelphia, Pennsylvania.
- MILLER, R. (1981): Kawazulite, $\text{Bi}_2\text{Te}_2\text{Se}$, related bismuth mineral and selenian covellite from the Northwest Territories. *Can. Mineral.* **19**, 341-348.
- MOH, G.H. (1969): The tin-sulfur system and related minerals. *Neues Jahrb. Mineral., Abh.* **111**, 227-263.
- MOLODKIN, A.K., IVLIEVA, V.I. & MESHCHERYAKOVA, E.V. (1979): Ordering in Sb_2Te_3 - Sb_2Se_3 solid solution. *Russ. J. Inorg. Chem.* **24**, 176-182.
- NEUMANN, G. & SCHEIDEGGER, R. (1967): Über die Existenz verschiedener Phasen im quasibinären System Bi_2S_3 - Bi_2S_3 . *Helv. Phys. Acta* **40**, 293-300.
- NODA, Y., OHBA, S., SATO, S. & SAITO, Y. (1983): Charge distribution and atomic thermal vibration in lead chalcogenide crystals. *Acta Crystallogr.* **B39**, 312-317.
- OLIVIER-FOURCADE, J., IBANEZ, A., JUMAS, J.C., MAURIN, M., LEFEBVRE, I., LIPPENS, P., LANNOO, M. & ALLAN, G. (1990): Chemical bonding and electronic properties in antimony chalcogenides. *J. Solid State Chem.* **87**, 366-377.
- PALKINA, K.K. & KUZNETSOV, V.G. (1965): Study of Sb_2Te_3 - Sb_2Se_3 alloys by X-ray and thermographic methods. *Russ. Inorg. Mater. (Izv. Akad. Nauk SSSR, Neorg. Mater.)* **1**, 2158-2164.
- PORTE, L. (1983): Diagrammes structuraux et liaison chimique dans les composés $\text{A}^{\text{NB}10-\text{N}}$. *J. Solid State Chem.* **46**, 64-75.
- ST. JOHN, J. & BLOCH, A.N. (1974): Quantum-defect electronegativity scale for nontransition elements. *Phys. Rev. Lett.* **33**, 1095-1098.
- SHANNON, R.D. & PREWITT, C.T. (1969): Effective ionic radii in oxides and fluorides. *Acta Crystallogr.* **B25**, 925-946.
- SMITH, M.J., KNIGHT, R.J. & SPENCER, C.W. (1962): Properties of Bi_2Te_3 - Sb_2Te_3 alloys. *J. Appl. Phys.* **33**, 2186-2190.
- SPRINGER, G. & LAFLAMME, J.H.G. (1971): The system Bi_2S_3 - Sb_2S_3 . *Can. Mineral.* **10**, 847-853.

- TIDESWELL, N.W., KRUSE, F.H. & MCCULLOUGH, J.D. (1957): The crystal structure of antimony selenide, Sb_2Se_3 . *Acta Crystallogr.* **10**, 99-102.
- VOUTSAS, G.P., PAPAZOGLU, A.G., RENTZEPERIS, P.J. & SIAPKAS, D. (1985): The crystal structure of antimony selenide, Sb_2Se_3 . *Z. Kristallogr.* **171**, 261-268.
- WELLS, A.F. (1984): *Structural Inorganic Chemistry* (5th ed.). Clarendon Press, Oxford, U.K.
- WIEDEMEIER, H. & VON SCHNERING, H.G. (1978): Refinement of the structures of GeS, GeSe, SnS and SnSe. *Z. Kristallogr.* **148**, 295-303.
- WOOLLEY, J.C. & BEROLO, O. (1968): Phase studies of the $\text{Pb}_{1-x}\text{Sn}_x\text{Se}$ alloys. *Mater. Res. Bull.* **3**, 445-450.

Received January 11, 1994, revised manuscript accepted June 15, 1994.